NACA RM E56J05

NACA

RESEARCH MEMORANDUM

PRELIMINARY INVESTIGATION OF METHODS TO INCREASE BASE PRESSURE OF PLUG NOZZLES AT MACH 0.9

By Reino J. Salmi

Lewis Flight Propulsion Laboratory
Cleveland, Ohio

NATIONAL ADVISORY COMMITTEE
FOR AERONAUTICS

WASHINGTON

December 19, 1956
Declassified October 31, 1958

4176

CJ-1

NATIONAL ADVISORY COMMITTEE FOR AERONAUTICS

RESEARCH MEMORANDUM

PRELIMINARY INVESTIGATION OF METHODS TO INCREASE BASE PRESSURE OF PLUG NOZZLES AT MACH 0.9

By Reino J. Salmi

SUMMARY

The effects of various afterbody changes on the net propulsive force of a nacelle-type plug nozzle installation were investigated at a Mach number of 0.9. The isentropic plug nozzle, which was designed for a jet pressure ratio of 15, was tested at jet pressure ratios up to 5. The results obtained are of a qualitative and comparative nature due to the omission of tunnel wall corrections and to estimates of jet-thrust losses. The data indicate that both a thin ring-type base shroud and a circular-arc boattail fairing were effective in increasing the net propulsive force to values greater than those for the basic cylindrical nacelle configuration. The ring shroud, which lengthened the nacelle but allowed free-stream air to bleed into the base area through a gap, was effective in reducing both the jet overexpansion and the nozzle base drag. The boattail fairing actually increased the total afterbody pressure drag (due to the necessary increase in the nacelle diameter) but was more effective in reducing the nozzle overexpansion by providing higher nozzle base pressures.

INTRODUCTION

The plug-type nozzle has exhibited very desirable thrust characteristics for large ranges of jet pressure ratio (e.g., ref. 1). The effects of external stream flow on the off-design performance of an isentropic plug nozzle (ref. 2) indicated that low pressures occurred on the nozzle base for certain type installations. In addition to creating a base drag, the low pressures caused an overexpansion of the jet, which reduced the plug thrust at lower-than-design jet pressure ratios.

The low base pressures occurred for the case where the nozzle was installed in a cylindrical nacelle. When a boattailed nacelle installation was used, the low base pressures were almost eliminated. The boattailed nacelles required a larger diameter, however, and the boattail drag as well as the forebody drag was not determined in those tests.

The present preliminary investigation was conducted to compare the pressure drags of boattailed installations of the isentropic plug nozzle as well as various types of shrouds which, when added to the original cylindrical nacelle, might increase the nozzle base pressures at little or no expense in drag.

The tests were conducted on small-scale models at a Mach number of 0.9.

4176

SYMBOLS

A area

C_D drag coefficient, D/q_0A_m

C_p pressure coefficient, $(p - p_0)/q_0$

C_F thrust coefficient, F/q_0A_m

D drag

F thrust

P total pressure

p static pressure

q dynamic pressure

r plug radius

x longitudinal distance from tip of plug

Subscripts:

b base

j jet

m basic model (configuration A)

0 free stream

4176

CJ-1 back

MODELS AND APPARATUS

The isentropic plug nozzle was designed for a jet pressure ratio of 15 which requires a nozzle lip or base angle of 37.1°, if all the expansion is external. In the basic nacelle installation (configuration A, fig. 1) the cylindrical body formed a sharp corner with the nozzle base. For one family of configurations (B, C, and E) the sharp corner at the base was preceded by a circular-arc boattail of 2.25 inches in radius. These configurations differed in the type of fairing ahead of the boattail. For configuration B, the maximum diameter extended forward for the full length of the body, whereas configurations C and E were faired to the basic nacelle diameter as shown in figure 1. Configuration E differed from configuration C in that a short straight section was included between the boattail and the conical flare. Configuration D was similar to configuration C except that the boattail radius was one-half that for configuration C. A photograph of configuration E is shown in figure 2.

The various ring shrouds and the boundary-layer scoop (configurations F to J) were soldered directly to configuration A or attached with four small brackets.

The models were installed in the 17.5-inch subsonic tunnel by extending the model through the bellmouth as shown in figure 3. Atmospheric air was drawn through the tunnel by an exhauster system. The pressure data were recorded photographically from multitube manometer boards. Included were the pressures on the faired afterbodies, the base, plug surface, and the tunnel wall, and the total pressure of the exiting jet. The tests were conducted at a nominal Mach number of 0.9 for jet pressure ratios of 2, 3, 4, and 5, in addition to the jet-off condition.

Wind tunnel wall corrections to the drag of the afterbody configurations were not applied in the present investigation. The usual corrections are based on the momentum change of the free-stream flow as it passes the afterbody to a uniform downstream pressure, and, therefore, account for the gross interference effect on the drag (ref. 3). A distribution of the interference effect to parts of the afterbody cannot be made, however, because the exact distribution of the interference is unknown. In the present case, the small-scale tests are of a comparative and exploratory nature. The maximum gross correction to the total afterbody drag coefficient would be an increase of less than 0.01 in the jet pressure ratio range of 4 to 5. The boattail and base would experience some fraction of this amount, which in itself is a small part of the total afterbody drag measured. In any case, if a correction were applied, it would be equal for all of the afterbody configurations tested since the base areas for all the configurations were equal.

RESULTS AND DISCUSSION

As pointed out earlier, the basic nacelle configuration suffers from low pressures on the base which causes overexpansion of the jet at lower-than-design jet pressure ratios in addition to high base drag. The effects of the various afterbody changes on the base pressure coefficient $C_{p,b}$ are presented in figure 4 as a function of the jet pressure ratio. In the present case, the effects are of most interest between jet pressure ratios of 3 and 5 which is the operating range of turbojet aircraft cruising at a Mach number of 0.9.

4176

As shown by figure 4, most of the afterbody changes increased the base pressure coefficient above the values for the cylindrical nacelle case (configuration A) at jet pressure ratios between 3 and 5. The greatest increase in $C_{p,b}$ was obtained with the extended boattail (configuration B), which is included in the investigation primarily for comparative purposes since the forebody drag due to increased nacelle diameter cannot be accounted for. The long bump (configuration E) which incorporated a short straight section ahead of the boattail was also very effective in increasing the base pressure. The long bump was considerably more effective than the boattail fairing (configuration C) which did not include the short straight section. The plain ring (configuration F) was the most effective of the shroud-type shields, and its effectiveness was exceeded only by the long bump and the extended boattail. The relatively poor performance of the boundary-layer diverter (configuration J) was unexpected and cannot be explained. The relative thickness of the boundary to the body diameter was representative of full-scale missile bodies (ref. 3).

The total afterbody drags of the more promising configurations are shown in figure 5. The lowest afterbody drag was obtained with the plain-ring shroud. Although it did not have the most favorable base pressure, the plain-ring shroud did not suffer from an added boattail or bump drag, which, in the case of the extended bump and extended boattail, actually increased the afterbody drag to values greater than those for the basic nacelle configuration. Although the drag of the ring shroud itself is not accounted for, it is believed to be insignificant because of its small projected area and short length.

The final evaluation of the various configurations depends, of course, on the net propulsive force, which includes the nozzle thrust minus the total afterbody drag. Normally the afterbody drag would include friction drag, but in the present case the friction drag was not evaluated. Unfortunately, the net propulsive force of the boattailed configurations cannot be obtained directly from the data. Slight errors in the plug position caused variations in the plug pressure distributions of the same order of magnitude as the differences in the jet thrust that would be sought. However, an indication of the relative values of the

4176

net propulsive force can be obtained from an estimation of the jet-thrust loss. As shown in reference 2, the jet-thrust loss increases with decreasing base pressure. To estimate this effect, a linear decrease in the jet thrust was assumed with decreasing base pressure. The jet-thrust loss at $C_{p,b}$ equal to zero is theoretically zero, and a measured value for the cylindrical nacelle case can be obtained from reference 2. The estimated thrust loss for the various afterbody configurations is shown in figure 6 as a nozzle thrust increment ΔC_F.

It can be seen from figure 6 that the boattail configurations have considerably lower nozzle thrust losses because of the favorable effects of higher base pressures. When the thrust decrement and the total afterbody drag are added, however, the disadvantage of the high boattail drags can again be noted as the lower propulsive force loss is obtained with the plain-ring-shroud configuration. The propulsive force loss of the extended boattail (configuration B) is lower than that of the extended bump (configuration E); however, it should be noted that the extended boattail configuration does not account for the additional forebody drag that would result from the increased nacelle diameter. It is interesting to note that for the basic nacelle configuration, the propulsive force loss at a jet pressure ratio of 5 would amount to approximately 12 percent of the net ideal thrust (where inlet momentum is considered) of a typical advanced turbojet engine (ref. 2). For the ring shroud this decrement would be less than 7 percent.

It is evident that much can be done to reduce the base drag and nozzle thrust loss that occur for the cylindrical nacelle-type plug nozzle installations. Additional research and development work are necessary to determine the optimum afterbody configurations from the viewpoint of net propulsive force. Larger scale models than those of the present tests should be used, however, to avoid the consequences of small errors in model geometry.

For the sake of providing qualitative design information on the bump configurations, the uncorrected pressure distributions over the afterbodies are presented in figure 7. It is interesting to note that although a net thrust force acted on the conical flared part of the afterbody bumps, the drag of the boattailed areas increased to a value greater than that for the extended boattail.

CONCLUDING REMARKS

Tests of various circular-arc boattail fairings and ring-type base shrouds on a cylindrical nacelle-type installation of a plug nozzle were made at a Mach number of 0.9. The results obtained are of a qualitative and comparative nature because of the omission of tunnel wall corrections and estimates of jet-thrust losses. The data indicate that:

1. A significant increase in the net propulsive force was obtained with either a circular boattail fairing or a ring-type base shroud.

2. The plain-ring shroud decreased both the total afterbody pressure drag and the jet-thrust loss due to overexpansion of the cylindrical nacelle installation. The boattailed configurations were more effective in increasing the base pressure and reducing the overexpansion losses but suffered from greater total afterbody drags because of the high drags of the boattail fairings.

4176

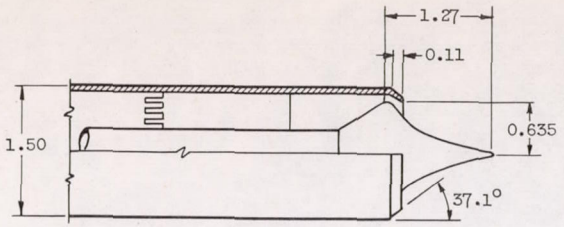
Lewis Flight Propulsion Laboratory
National Advisory Committee for Aeronautics
Cleveland, Ohio, October 15, 1956

REFERENCES

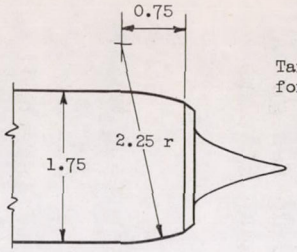
1. Krull, H. George, and Beale, William T.: Effect of Plug Design on Performance Characteristics of Convergent-Plug Exhaust Nozzles. NACA RM E54H05, 1954.

2. Salmi, R. J., and Cortright, E. M., Jr.: Effects of External Stream Flow and Afterbody Variations on the Performance of a Plug Nozzle at High Subsonic Speeds. NACA RM E56F11a, 1956.

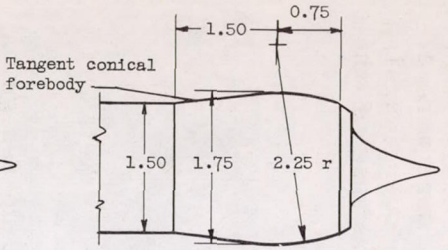
3. Salmi, Reino J.: Experimental Investigation of Drag of Afterbodies with Exiting Jet at High Subsonic Mach Numbers. NACA RM E54I13, 1954.



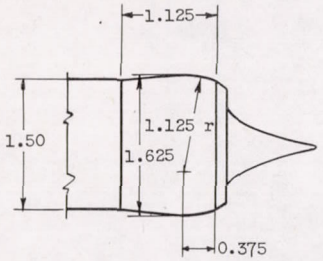
Configuration A, cylindrical body



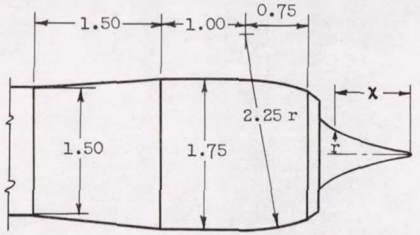
Configuration B, extended boattail



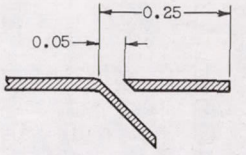
Configuration C, large bump



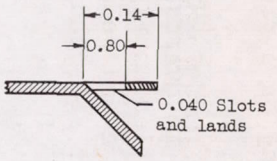
Configuration D, small bump



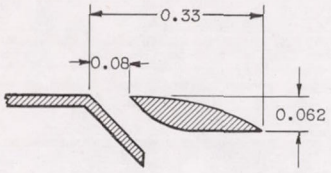
Configuration E, extended bump



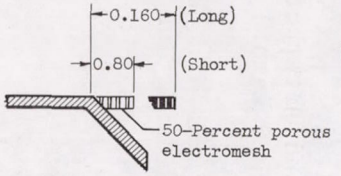
Section F, plain ring



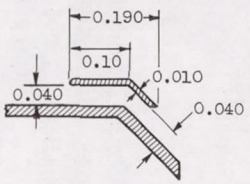
Section G, slotted ring



Section H, contoured ring



Section I, porous rings:
(Short ring, configuration I_a;
long ring, configuration I_b)



Section J,
boundary-layer diverter

Plug coordinates			
X	r	X	r
0	0.023	1.20	0.556
.2	.059	1.25	.570
.4	.105	1.27	.573
.6	.172	1.30	.569
.75	.235	1.35	.551
.90	.319	1.55	.435
1.05	.425	1.80	.290
1.15	.517		

CD-5352

Figure 1. - Geometry of models. (All dimensions in inches except where noted.)

4176

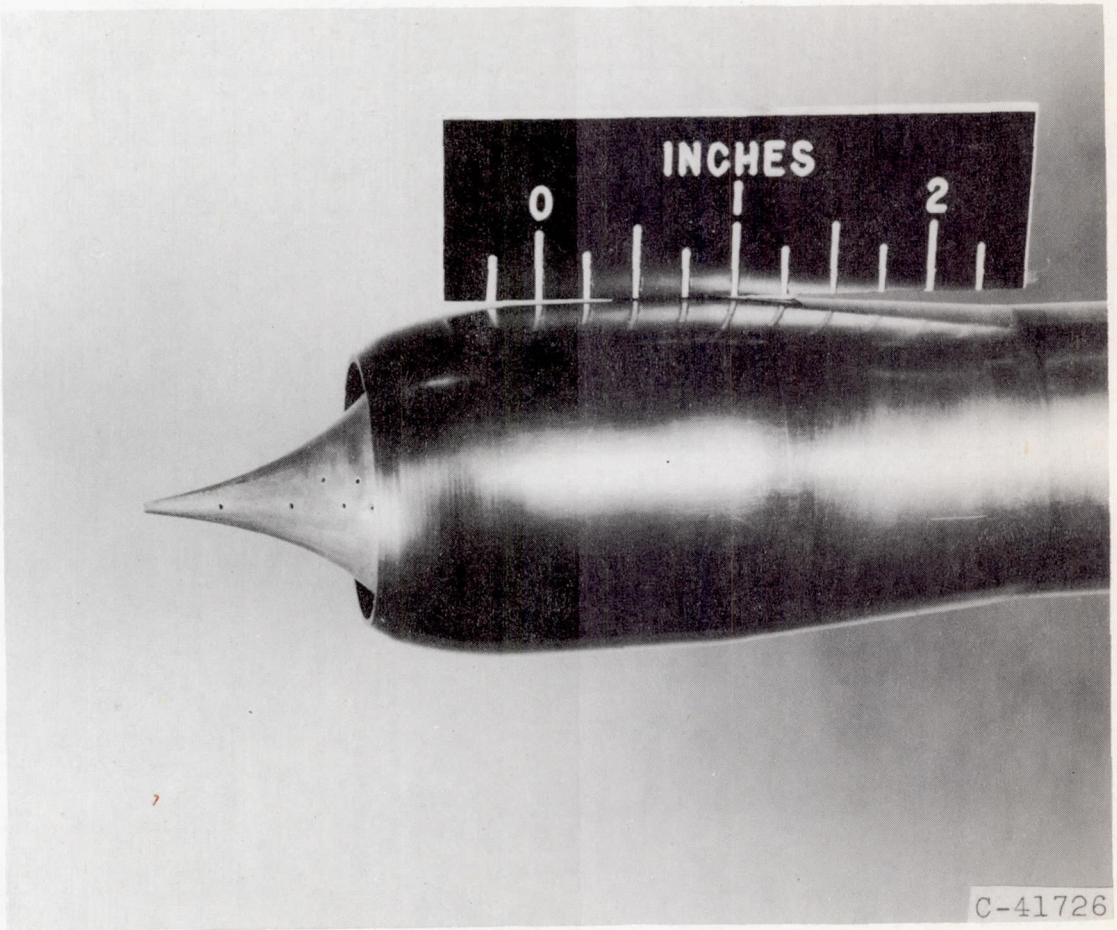


Figure 2. - Photograph of configuration E.

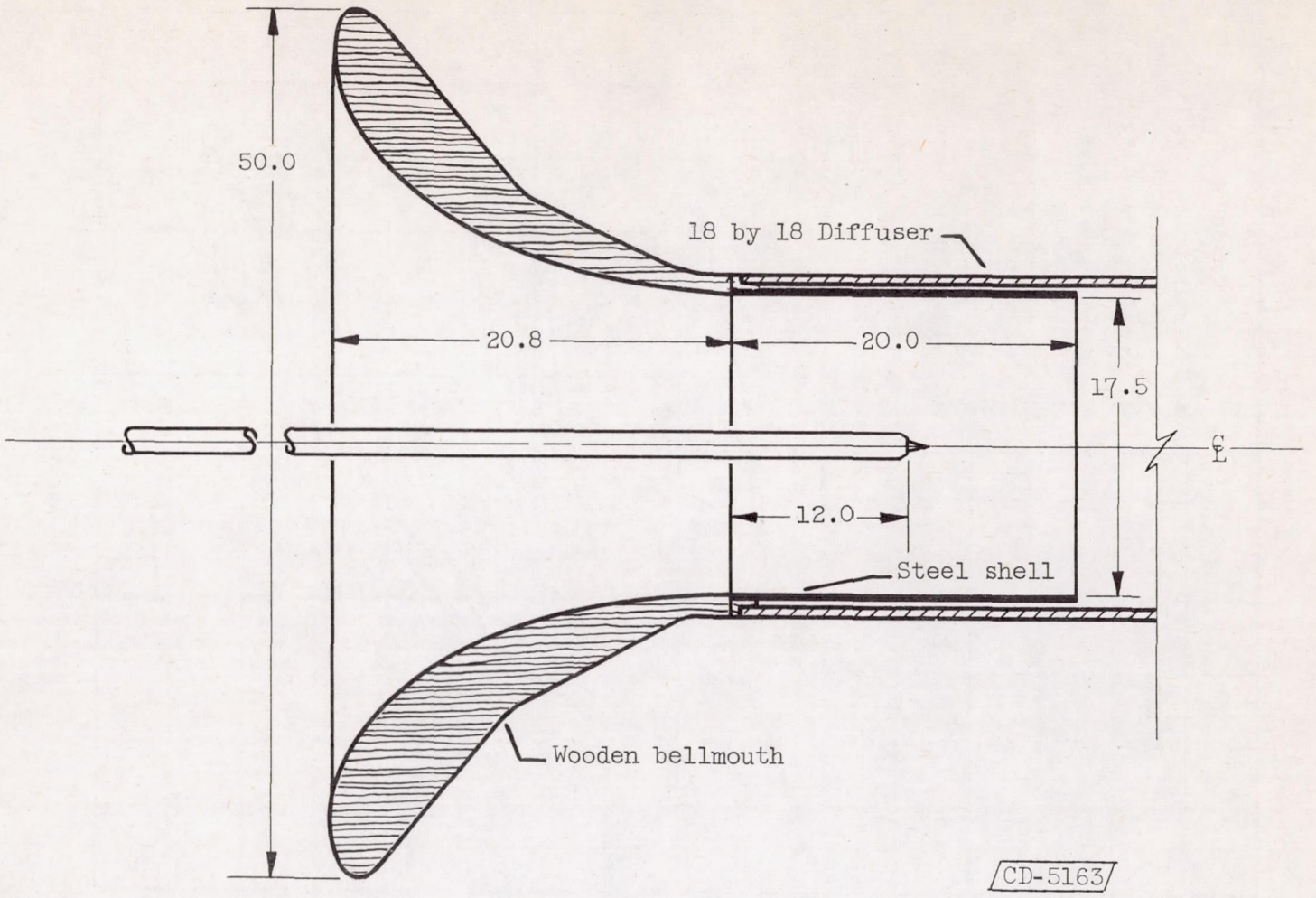


Figure 3. - Schematic diagram of tunnel and model. (All dimensions in inches.)

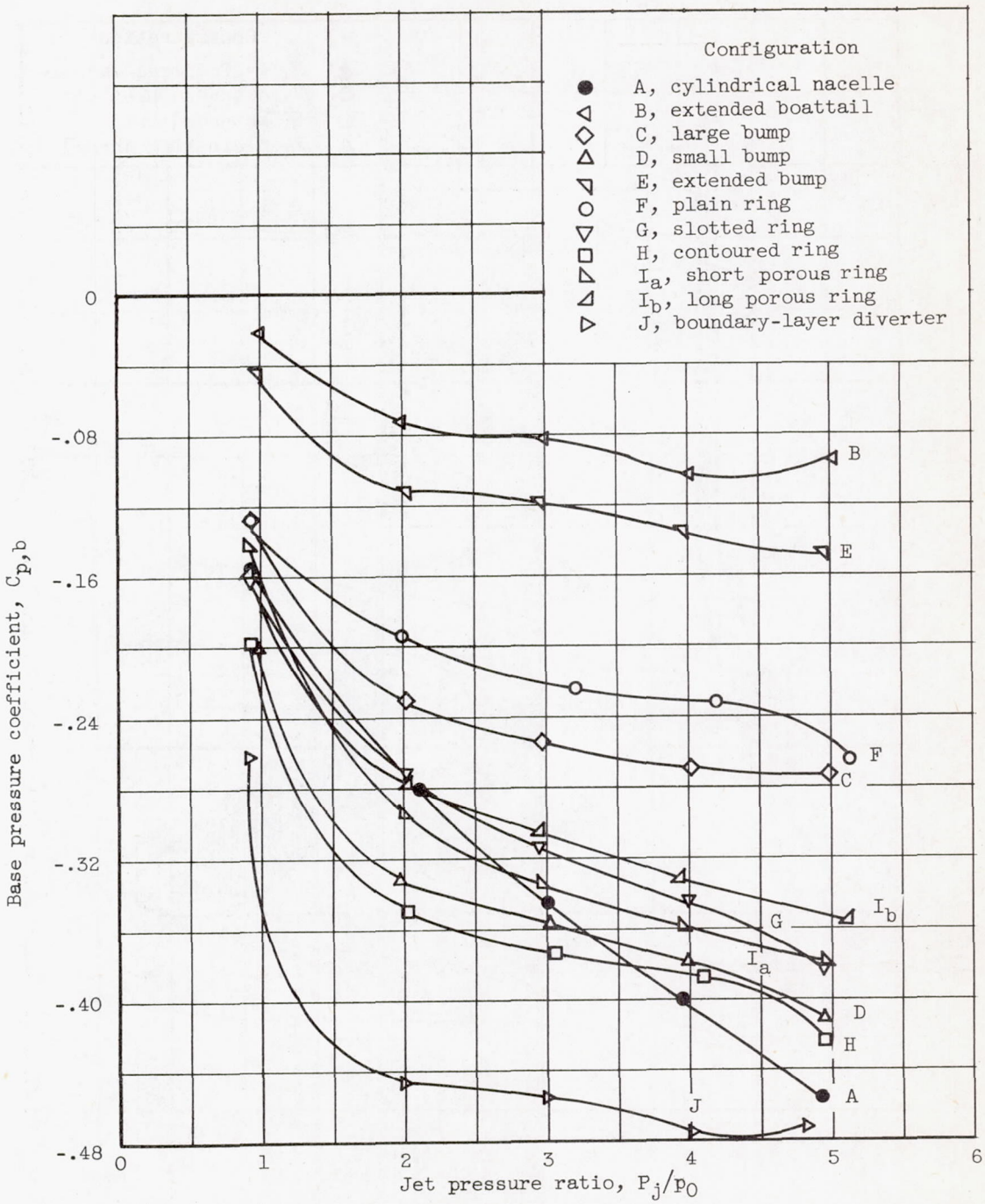
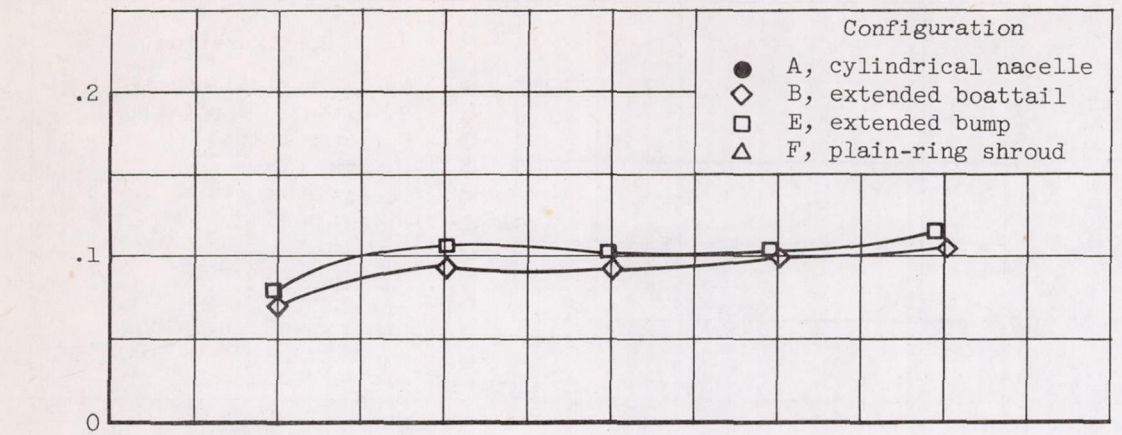
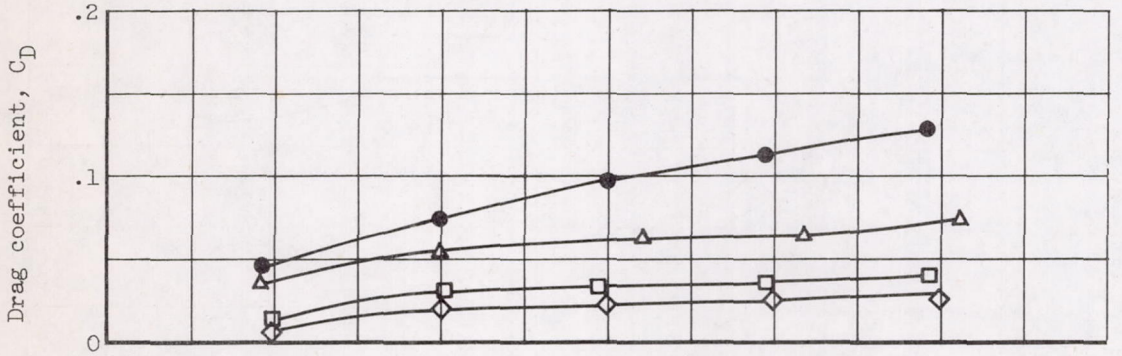


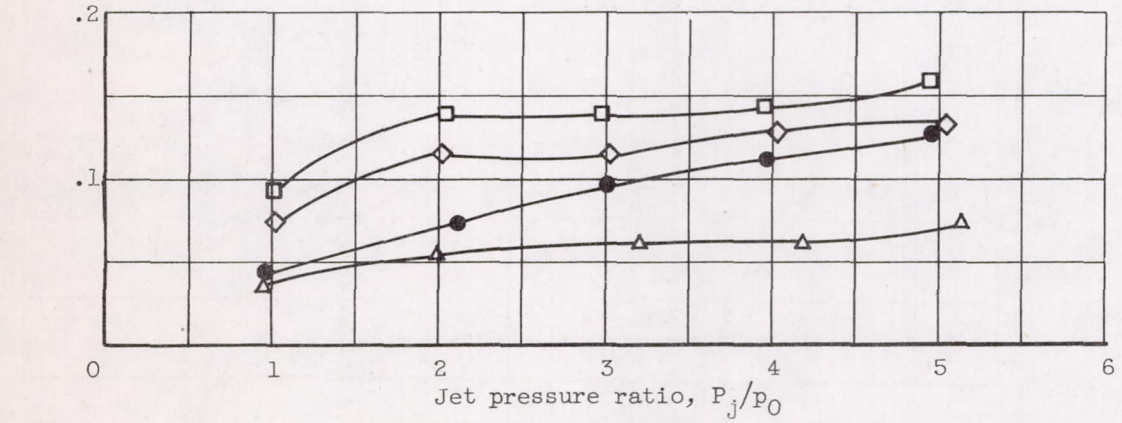
Figure 4. - Effect of various afterbody configurations on plug nozzle base pressure coefficient. Free-stream Mach number, 0.9.



(a) Boattail drag.



(b) Base drag.



(c) Total afterbody drag.

Figure 5. - Total and component drags of various configurations.

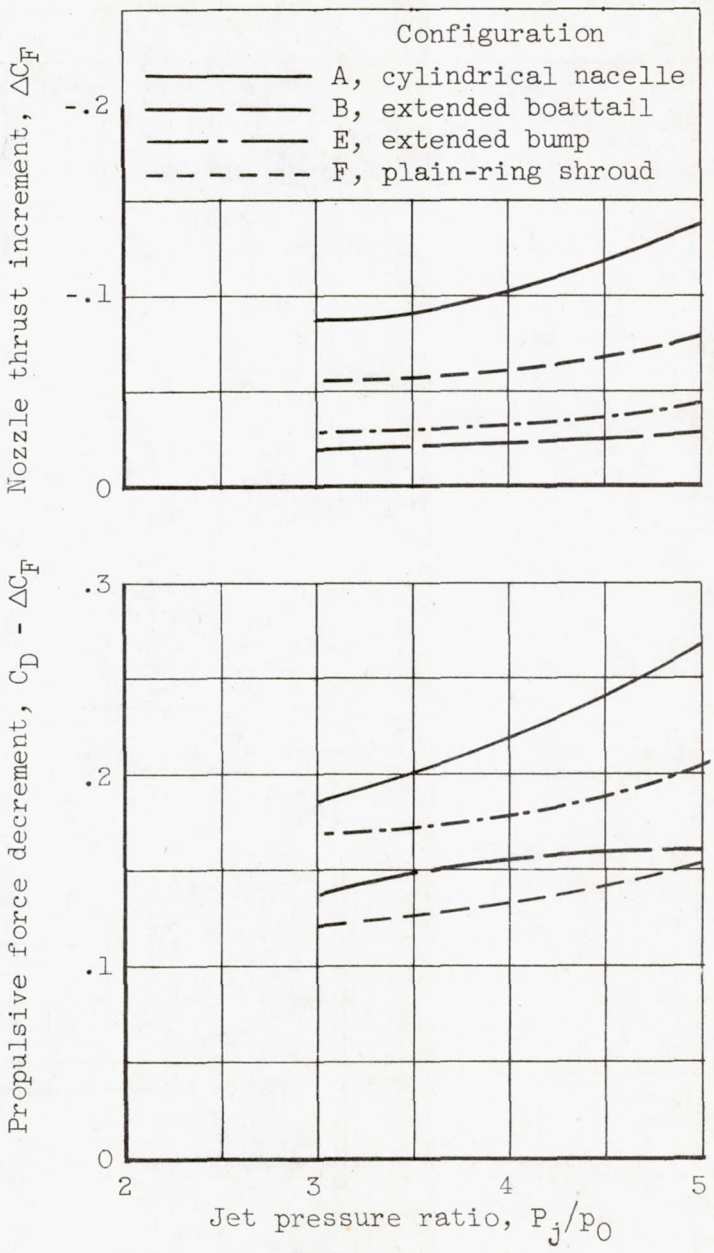


Figure 6. - Estimated jet-thrust loss and propulsive force decrement.

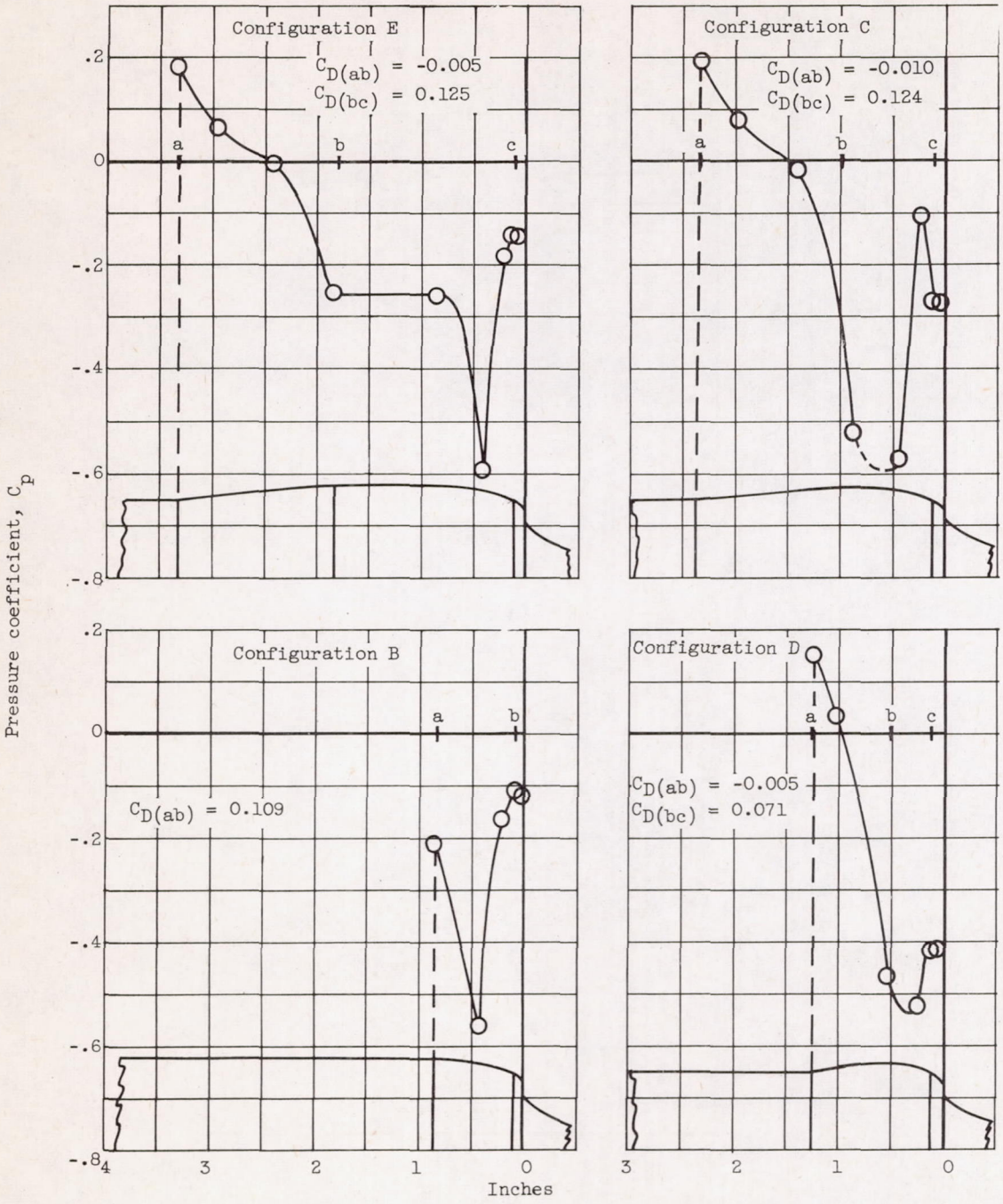


Figure 7. - Pressure distributions for various bump afterbodies. Jet pressure ratio, 5; free-stream Mach number, 0.9.